A&A 554, A44 (2013)
DOI: 10.1051/0004-6361/201321520

Astronomy & Astrophysics

Kinematics and chemical properties of the Galactic stellar populations⋆

The HARPS FGK dwarfs sample

V. Zh. Adibekyan[1], P. Figueira[1], N. C. Santos[1,2], A. A. Hakobyan[3,4], S. G. Sousa[1,5], G. Pace[1], E. Delgado Mena[1], A. C. Robin[6], G. Israelian[5,7], and J. I. González Hernández[5,7]

[1] Centro de Astrofísica da Universidade do Porto, Rua das Estrelas, 4150-762 Porto, Portugal
e-mail: Vardan.Adibekyan@astro.up.pt
[2] Departamento de Física e Astronomia, Faculdade de Ciências da Universidade do Porto, 4169-007 Porto, Portugal
[3] Byurakan Astrophysical Observatory, 0213 Byurakan, Aragatsotn province, Armenia
[4] Isaac Newton Institute of Chile, Armenian Branch, 0213 Byurakan, Aragatsotn province, Armenia
[5] Instituto de Astrofísica de Canarias, 38200 La Laguna, Tenerife, Spain
[6] Institut Utinam, CNRS UMR 6213, Université de Franche-Comté, OSU THETA de Franche-Comté-Bourgogne, 25010 Besançon, France
[7] Departamento de Astrofísica, Universidad de La Laguna, 38206 La Laguna, Tenerife, Spain

Received 20 March 2013 / Accepted 8 April 2013

ABSTRACT

Aims. We analyzed chemical and kinematical properties of about 850 FGK solar neighborhood long-lived dwarfs observed with the HARPS high-resolution spectrograph. The stars in the sample have $\log g \geq 4$ dex, $5000 \leq T_{\rm eff} \leq 6500$ K, and $-1.39 \leq$ [Fe/H] ≤ 0.55 dex. The aim of this study is to characterize and explore the kinematics and chemical properties of stellar populations of the Galaxy in order to understand their origins and evolution.

Methods. We applied a purely chemical analysis approach based on the [α/Fe] vs. [Fe/H] plot to separate Galactic stellar populations into the thin disk, thick disk, and high-α metal-rich (hαmr). Then, we explored the population's stellar orbital eccentricity distributions, their correlation with metallicity, and rotational velocity gradients with metallicity in the Galactic disks to provide constraints on the various formation models.

Results. We identified a gap in the [α/Fe]–[Fe/H] plane for the α-enhanced stars, and by performing a bootstrapped Monte Carlo test we obtained a probability higher than 99.99% that this gap is not due to small-number statistics. Our analysis shows a negative gradient of the rotational velocity of the thin disk stars with [Fe/H] (–17 km s^{-1} dex^{-1}), and a steep positive gradient for both the thick disk and hαmr stars with the same magnitude of about +42 km s^{-1} dex^{-1}. For the thin disk stars we observed no correlation between orbital eccentricities and metallicity, but observed a steep negative gradient for the thick disk and hαmr stars with practically the same magnitude ($\approx$–0.18 dex^{-1}). The correlations observed for the nearby stars (on average 45 pc) using high-precision data, in general agree well with the results obtained for the SDSS sample of stars located farther from the Galactic plane.

Conclusions. Our results suggest that radial migration played an important role in the formation and evolution of the thin disk. For the thick disk stars it is not possible to reach a firm conclusion about their origin. Based on the eccentricity distribution of the thick disk stars only their accretion origin can be ruled out, and the heating and migration scenario could explain the positive steep gradient of V_ϕ with [Fe/H]. When we analyzed the hαmr stellar population we found that they share properties of both the thin and thick disk population. A comparison of the properties of the hαmr stars with those of the subsample of stars from the N-body/SPH simulation using radial migration suggest that they may have originated from the inner Galaxy. Further detailed investigations would help to clarify their exact nature and origin.

Key words. stars: abundances – stars: kinematics and dynamics – Galaxy: disk

1. Introduction

The formation and evolution of the Galactic disks is an important topic in contemporary astrophysics. The Milky Way (MW) has a composite and complex structure with several main components (halo, bulge, thin disk, and thick disk) and many stellar streams whose origins are far from being thoroughly understood.

The three main stellar populations of the MW in the solar neighborhood are the thin disk, the thick disk, and the halo, although most of these stars belong to the thin and thick disks. The subdivision between the thick disk and thin disk was first identified by Gilmore & Reid (1983), who analyzed the stellar density distribution as a function of distance from the Galactic plane. These two populations have different kinematics and chemical properties. Generally, the thick disk is thought to be composed of relatively old stars (e.g., Bensby et al. 2003, 2005; Fuhrmann 2008; Adibekyan et al. 2011), metal-poor, and α-enhanced (e.g., Fuhrmann 1998, 2008; Prochaska et al. 2000; Feltzing et al. 2003; Reddy et al. 2006; Haywood 2008; Lee et al. 2011; Adibekyan et al. 2012) that move in Galactic orbits with a large-scale height and long-scale length (e.g., Robin et al. 1996; Buser et al. 1999; Jurić et al. 2008; Kordopatis et al. 2011). However, some of the observed trends may depend on the criteria applied to divide stars into the two disk populations (e.g., Fuhrmann 2008; Schönrich & Binney 2009b; Lee et al. 2011). Interestingly, this model has recently been challenged. Recent analyses of the geometric decompositions of the Galactic disk based on the

⋆ Based on observations collected at the La Silla Paranal Observatory, ESO (Chile) with the HARPS spectrograph at the 3.6-m telescope (ESO runs ID 72.C-0488, 082.C-0212, and 085.C-0063).

elemental-abundance selection of the sample stars yielded strikingly different results (see Bovy et al. 2012a,b; Liu & van de Ven 2012). Bovy et al. (2012a) find that mass-weighted scale-height distribution smoothly varies and that there is no thin-thick disk bi-modality (i.e., the MW has no distinct thick disk). We refer the reader to Ivezić et al. (2012) and Rix & Bovy (2013) for more recent reviews of the stellar disk(s) and populations.

While considering that the thick disk was formed by one single mechanism is most probably too semplicistic, several different scenarios have been proposed for the formation of thick disk: the heating of a pre-existing old thin disk via minor mergers (e.g., Quinn et al. 1993; Villalobos & Helmi 2008), the direct accretion of stars from disrupted satellites (e.g., Abadi et al. 2003), gas accretion at high redshift and stars formed in situ (e.g., Brook et al. 2005), and radial migration of stellar orbits (e.g., Schönrich & Binney 2009a,b; Loebman et al. 2011).

The proposed scenarios offer very different observationally testable signatures, hence certain well-defined properties of the Galactic disks should be able to distinguish between these possible scenarios. In this paper, to provide constraints on the various suggested formation models, we explore the stellar orbital eccentricity distributions (e.g., Sales et al. 2009; Di Matteo et al. 2011), a possible correlation between the eccentricities and metallicity (see Lee et al. 2011), and rotational velocity gradients with metallicity in the thin and thick disks (e.g., Lee et al. 2011; Kordopatis et al. 2011; Navarro et al. 2011; Liu & van de Ven 2012).

For our analyses we used the stellar sample of 1111 long-lived FGK dwarf stars from Adibekyan et al. (2012). To separate and characterize the different Galactic stellar subsystems, we focus on the [α/Fe] ratio (here α refers to the average abundance of Mg, Si, and Ti).

The outline of this paper is as follows: in Sect. 2 we introduce the sample and present the chemical criteria of the disks deviation. Results and discussion of comparisons of our results with the predictions of different contemporary disk formation scenarios follow in Sect. 3. Finally, in Sect. 4, we draw our main conclusions.

2. The sample and disk definition

It is becoming increasingly clear that a dissection of the Galactic disks based only on stellar abundances is superior to kinematic separation (e.g., Navarro et al. 2011; Lee et al. 2011; Adibekyan et al. 2011; Liu & van de Ven 2012). This is because chemistry is a relatively more stable property of a star than its spatial positions and kinematics. In this analysis, to separate the thin – and thick disk stellar components, we used the position of the stars in the [α/Fe]–[Fe/H] plane.

2.1. Sample selection and stellar parameters

Our initial sample comprises 1111 FGK dwarfs with high-resolution spectra observed with the HARPS spectrograph (Mayor et al. 2003) at the ESO 3.6-m telescope (La Silla, Chile). It is a combination of three HARPS subsamples, HARPS-1 (Mayor et al. 2003); HARPS-2 (Lo Curto et al. 2010); and HARPS-4 (Santos et al. 2011). The HARPS-1 is composed of 451 stars, 376 of which have been selected from the CORALIE volume-limited sample[1] (Udry et al. 2000) because they are non-active and low-rotating, and the rest are southern confirmed exoplanetary host stars. The HARPS-2 sample was compiled with stars in the solar neighborhood out to 57.5 pc from the Sun (Lo Curto et al. 2010) to complete a planet-search survey previously started with the CORALIE spectrograph. Active, high-rotating, known binaries and variable stars were then excluded which brought the sample to 582 stars (Sousa et al. 2011b). It is worth noting, that for the CORALIE sample a color cut-off ($B - V < 1.2$) was made. The HARPS-4 sample consists of 97 stars and was compiled from the catalog of Nordström et al. (2004), selecting stars with $b - y > 0.33$ and with photometric [Fe/H] between –1.5 and –0.5 dex (Sousa et al. 2011a). We note that there are four stars in common between HARPS-1 and HARPS-4, and 14 stars in common between the HARPS-2 and HARPS-4 subsamples.

Precise stellar parameters ($T_{\rm eff}$, log g, [Fe/H], and $\xi_{\rm t}$) and elemental abundances for 12 elements (Na, Mg, Al, Si, Ca, Ti, Cr, Ni, Co, Sc, Mn, and V) for all the stars were determined in a homogeneous manner. Briefly summarizing, the equivalent widths of the lines were automatically measured with the ARES[2] code (Automatic Routine for line Equivalent widths in stellar Spectra, Sousa et al. 2007). The atmospheric parameters and elemental abundances were then determined using a local thermodynamic equilibrium (LTE) analysis relative to the Sun with the 2010 revised version of the spectral synthesis code MOOG[3] (Sneden 1973) and a grid of Kurucz ATLAS9 plane-parallel model atmospheres (Kurucz 1993). The reference abundances used in the abundance analysis were taken from Anders & Grevesse (1989). We refer the reader to Adibekyan et al. (2012) and Sousa et al. (2008) for more details.

In order to assemble a sample of stars with the most reliable and precise abundance determinations, we decided to establish a cutoff in temperature: we excluded stars with $T_{\rm eff} \leq 5000$ K and $T_{\rm eff} \geq 6500$ K. In these temperature regions the errors, both in stellar parameters and [X/H] abundances, are higher (see Neves et al. 2009; Sousa et al. 2011a,b; Adibekyan et al. 2012; Tsantaki et al. 2013, for more details). At the end of the establishing cutoff on temperature we finished with 869 stars. Since we are interested in long-lived dwarfs, we excluded stars with log $g \leq 4$ dex (23 stars), leading to a final sample of 846 stars.

Our final sample spans the metallicity range $-1.39 \leq$ [Fe/H] ≤ 0.55 dex, although there are only nine stars with [Fe/H] < –0.9 dex, and two stars with [Fe/H] > 0.4 dex. The typical relative uncertainties in the metallicity and [α/Fe] are of about 0.03 dex (see Adibekyan et al. 2012).

2.2. Dissecting the Galactic disks

As mentioned above, the thin- and thick disk stars are different in their α content at a given metallicity ([Fe/H]). Here we use this dichotomy in the chemical evolution to separate different stellar populations.

Adibekyan et al. (2011) showed that the stars of this sample fall into two populations, clearly separated in terms of [α/Fe] up to super-solar metallicities. In turn, high-α stars were also separated into two families with a gap in both [α/Fe] and metallicity ([α/Fe] ≈ 0.17 dex and [Fe/H] ≈ -0.2 dex) distributions. Here we use the same technique as in Adibekyan et al. (2011) to separate the stellar groups[4].

[1] The limit distance for the stars in this sample depends on the stellar spectral type, i.e., a color-dependent distance cutoff was applied.

[2] The ARES code can be downloaded from http://www.astro.up.pt/sousasag/ares

[3] The source code of MOOG can be downloaded from http://www.as.utexas.edu/~chris/moog.html

[4] We note that in the current analysis we established a more conservative temperature cutoff than in our previous work.

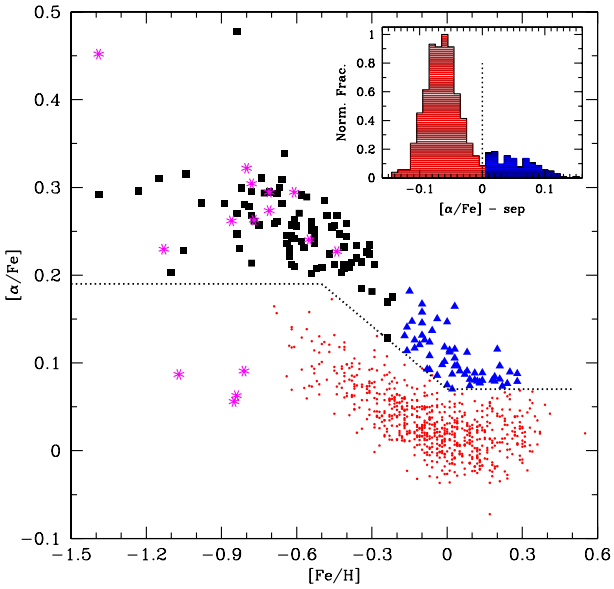

Fig. 1. [α/Fe] vs. [Fe/H] for the whole sample. Magenta asterisks represent the stars belonging to the halo by their kinematics. The black dotted line is the fiducial for division into thin- and thick disk populations. The black filled squares refer to the thick disk stars, blue triangles to the hαmr, and the red dots to the thin disk stars. On the top-right corner we plot the histogram of the distribution of [α/Fe], after the fiducial model (separation curve) is subtracted.

The [α/Fe] vs. [Fe/H] separation plot for the sample stars is depicted in Fig. 1. The histogram (right-top corner) shows that the separation between the stellar families (low-α and high-α) is clear. Many recent papers separate the thin and thick disk stars by the [α/Fe] gap at ≈0.2–0.3 dex (see Navarro et al. 2011; Lee et al. 2011) and other papers also report the existence of the knee in [α/Fe] trends for the thick disk stars (kinematically selected) when [Fe/H] reaches to ≈–0.3 dex (e.g., Feltzing et al. 2003; Bensby et al. 2007). A similar gap in [α/Fe] at ≈0.2 dex and similar downturn in [Fe/H] at ≈–0.3 dex are seen in Fig. 1, and as already noted, there is also a gap between metal-poor and metal-rich α-enhanced stars (the gap in [Fe/H] can be seen in the top-left panel of Fig. 2). We note that there is no [Fe/H] gap found for the thin disk stars. The presence of a metal-rich, old thick disk is already noticed in the spectroscopic studies of Feltzing & Bensby (2008) and Casagrande (2012), and a metal-rich α-rich population has also been recently confirmed by Gazzano et al. (2013).

In the [Fe/H] region from –0.28 to –0.18 dex there are only three stars with enhanced α abundances, while at lower and higher metallicities the number of α-enhanced stars is higher (9 and 13, respectively). In order to analyze whether this lack of high-α stars in the mentioned region is statistically significant or is due to a small-number statistics, we performed a simple bootstrapped Monte Carlo test. We randomly selected 119 stars, which is the number of high-α stars in the metallicity region $-0.7 \leq$ [Fe/H] ≤ 0.3 dex, from our sample in the same metallicity region (independent from their α content). Then we counted the number of stars in the interested metallicity region, from –0.28 to –0.18 dex. We also varied this interval by 0.05 dex ([–0.33; –0.23] to [–0.23; –0.13]). The entire process was repeated 10^5 times. This test indicates that such a small amount of stars in the –0.28 to –0.18 dex metallicity region (or in the above mentioned intervals) can be obtained by chance with less than 0.01% probability for four (or fewer) stars, and 0.05% probability for five (or fewer) stars. In our simulation we had only one case where the mentioned metallicity interval contained three or fewer stars (0.001%). This Monte Carlo test indicates that it is very unlikely that the observed gap between metal-poor and metal-rich α-enhanced stars is due to small-number statistics and therefore the separation is considered real.

As mentioned before, our sample consists of three HARPS subsamples, one of which (HARPS-4) was built to include only metal-poor stars. Keeping this in mind, one might suspect that the observed gap could be a result of the over-sampling of a thick disk metallicity distribution. However, this can not be the case, because our thick disk sample includes only 32 stars from HARPS-4, and almost all of them have metallicities below –0.5 dex; there is only one star with [Fe/H] > –0.4 dex, and two stars with $-0.5 <$ [Fe/H] < -0.4 dex.

The magenta asterisks in Fig. 1 refer to stars belonging to the halo selected by their kinematics (see Adibekyan et al. 2011). As is clearly evident, halo stars are divided into two high-α and low-α groups. This dichotomy confirms the results already found by Nissen & Schuster (2010).

2.3. Characterization of the Galactic components

Guided by the chemical separation, we can characterize the stellar families in terms of their kinematics and metallicity. Figure 2 shows the distributions of the $U_{\rm LSR}$, $V_{\rm LSR}$, and $W_{\rm LSR}$ space velocity components relative to the local standard of rest (LSR) and iron abundance for our stellar groups. For details of the computation of the space velocity components we refer the reader to Adibekyan et al. (2012). In the plot we also separately present the distributions of the thick disk + hαmr sample stars, because the link between these two stellar groups is still under debate (see Sect. 3). The average values of the [Fe/H] and $U_{\rm LSR}$, $V_{\rm LSR}$, and $W_{\rm LSR}$ velocity components and their standard deviations, along with their fractions, are presented in Table 1. We also performed Gaussian fits of the distributions of $U_{\rm LSR}$, $V_{\rm LSR}$, $W_{\rm LSR}$, and [Fe/H] for each Galactic component, and present the mean values and dispersion in the same table (the values in brackets). We did not perform Gaussian fitting for the halo stars because of the small number of stars in this group. We also did not fit [Fe/H] distribution of thick disk + hαmr family, because the distribution is obviously bimodal and cannot be fitted with one Gaussian.

From Fig. 2 and the corresponding table it is obvious that the velocity distributions of the hαmr stars are intermediate (even more similar to those of the thin disk stars) between thin and thick disk population stars (see also Adibekyan et al. 2011), but with their average velocities and standard deviations having intermediate values between the thin and thick disk families. The Kolmogorov-Smirnov (K-S) statistics predict 0.52, 0.01, and 0.02 probabilities ($P_{\rm KS}$) that hαmr and thin disk stars come from the same underlying distribution for $U_{\rm LSR}$, $V_{\rm LSR}$, and $W_{\rm LSR}$. The same statistical test gives much lower probabilities when we compare the velocity distributions of the hαmr and thick disk stars – $U_{\rm LSR}$ ($P_{\rm KS} \approx 0.38$), $V_{\rm LSR}$ ($P_{\rm KS} \approx 3 \times 10^{-5}$), and $W_{\rm LSR}$ ($P_{\rm KS} \approx 0.005$). From the plot it can be noted that the velocity distributions of the thick disk stars are not perfectly Gaussian. This can be seen also from Table 1 where the arithmetic averages (and rms) and means of the Gaussian fits (and standard deviations) are different. The kinematic parameters obtained for the thin and thick disks, in general, agree well with those obtained for kinematically selected thin and thick disks in the solar neighborhood (e.g., Bensby et al. 2003; Soubiran et al. 2003; Robin et al. 2003), but local normalization for the thick disk is a bit higher (but see also Soubiran et al. 2003; Mishenina et al. 2004; Kordopatis et al. 2011). For illustrative purposes as

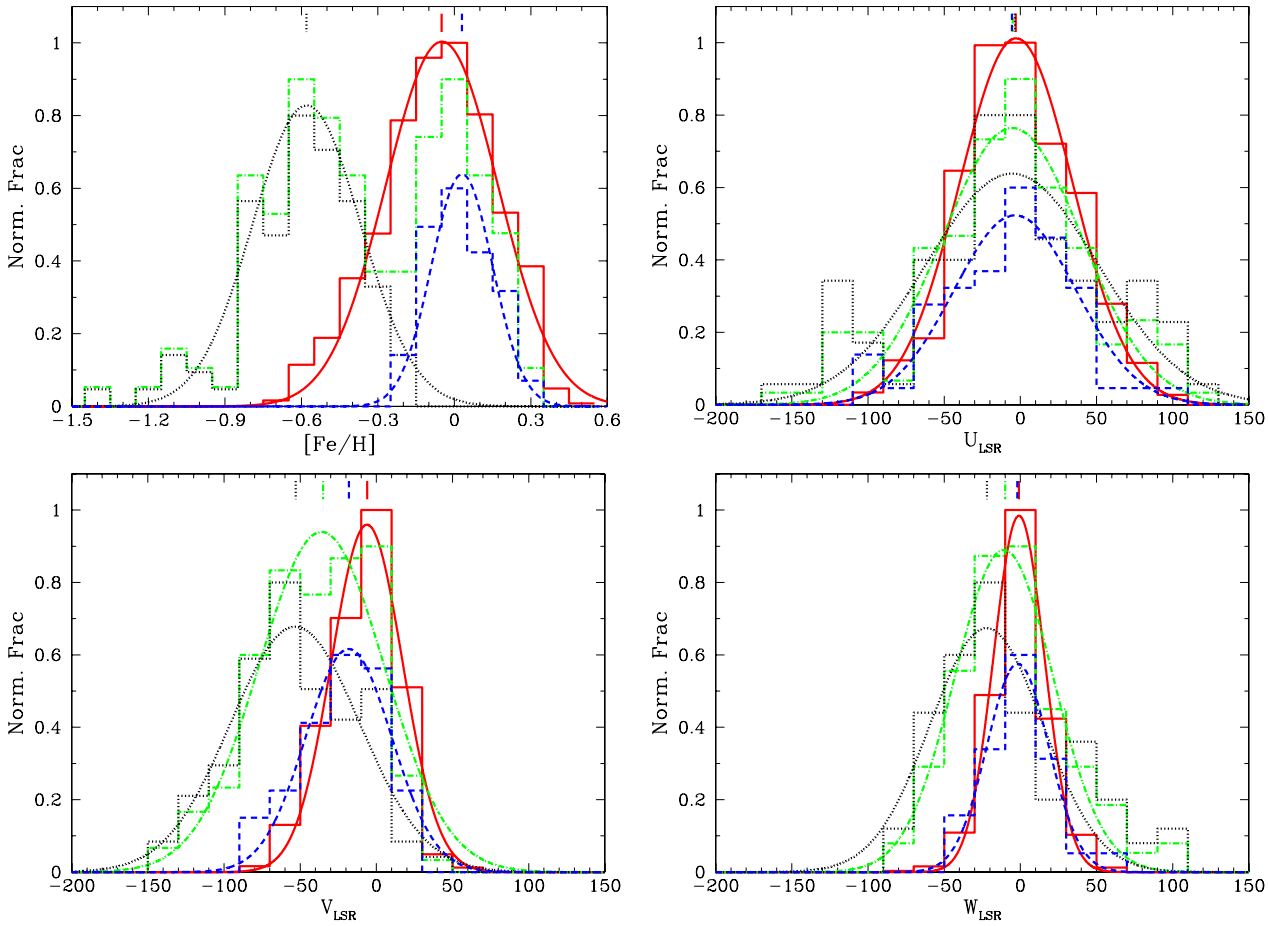

Fig. 2. Distributions of the Galactic space velocities and metallicity of the stars from the thick disk (black dotted), hαmr (blue dashed), the thin disk (red solid), and the thick disk + hαmr (green dot-dashed). Gaussian fits of the data are also presented. The mean of Gaussian fits is shown by vertical lines at the top of each distribution. Note that the distributions of different groups were set lower or higher for the sake of clarity.

Table 1. The average values of the U_{LSR}, V_{LSR}, and W_{LSR} velocity components and their standard deviations for the stellar groups, along with the number of stars and their percentages.

Stellar groups	U_{LSR}	σ_U	V_{LSR}	σ_V	W_{LSR}	σ_W	[Fe/H]	N	Percentage
Thick	–5(–5)	66(56)	–52(–53)	39(42)	–8(–22)	44(36)	–0.60 ± 0.23(–0.58)	84	9.94 ± 1.03
hαmr	–7(–3)	42(39)	–23(–18)	26(28)	0(–2)	21(20)	0.03 ± 0.12(0.03)	58	6.85 ± 0.86
Thick+hαmr	–6(–5)	58(45)	–40(–35)	37(41)	–4(–10)	36(32)	–0.34 ± 0.37	142	16.78 ± 1.28
Thin	0(–3)	37(37)	–9(–6)	22(23)	0(–1)	18(16)	–0.06 ± 0.22(–0.05)	692	81.79 ± 1.32
Halo	–39	154	–198	60	–27	73	–0.82 ± 0.23	12	1.42 ± 0.40

Notes. The values obtained from the Gaussian fittings of the data is presented in brackets.

a complement to Fig. 2, the distribution of stars of our sample in the Toomre diagram is shown in Fig. 3.

Although in Table 1 we present the average values of the velocities and metallicity obtained for halo stars, we note that these values should be considered with caution because the number of stars in the sample is very low.

3. Results and discussion

As mentioned in the Introduction, several scenarios have been proposed for the formation of the Galactic disks that could have left different dynamical and chemical imprints. In this section we test the predictions of the mentioned scenarios using our sample of local thin and thick disk FGK dwarfs as identified above. At the end of the section we discuss the main properties of the hαmr stellar family.

3.1. Rotational velocity and metallicity

The large dispersion in the metallicities of the thin disk stars in the solar neighborhood, according to the migration-based scenarios (Sellwood & Binney 2002; Roškar et al. 2008; Schönrich & Binney 2009a; Minchev & Famaey 2010), can be explained by inward radial migration of metal-poor and outward migration of metal-rich stars. A consequence of the radial migration is a negative correlation between rotational velocities (V_ϕ) and metallicity (Schönrich & Binney 2009a; Loebman et al. 2011) for the thin disk (low-[α/Fe]) stars. We note that this prediction is not an exclusive to radial migration, models that assumed inside-out formation can also produce this anti-correlation. This trend in the young stars arises from epicyclic motions of stars with their birth radii imprinted into their metallicities and disappears with time as a result of complete mixing. Hence, the same models predict

Table 2. Observed gradients, correlation coefficients of V_ϕ and eccentricity with metallicity, the number of stars, and significance of the correlation for different stellar populations.

Stellar groups	$\partial V_\phi/\partial$[Fe/H] (km s^{-1} dex^{-1})	$r_{\partial V_\phi/\partial[Fe/H]}$	$N(V_\phi)$	$n\sigma(V_\phi)$	$\partial e/\partial$[Fe/H] (dex^{-1})	$r_{\partial e/\partial[Fe/H]}$	$N(e)$	$n\sigma(e)$
Thick	41.9 ± 18.1	0.247	84	2.24σ	–0.184 ± 0.078	–0.266	73	2.24σ
hαmr	41.4 ± 28.2	0.190	58	1.43σ	–0.185 ± 0.138	–0.212	40	1.30σ
Thick+hαmr	43.9 ± 7.6	0.435	142	5.19σ	–0.208 ± 0.036	–0.475	113	5.27σ
Thin	–16.8 ± 3.7	–0.164	692	4.43σ	–0.023 ± 0.015	–0.212	515	4.81σ

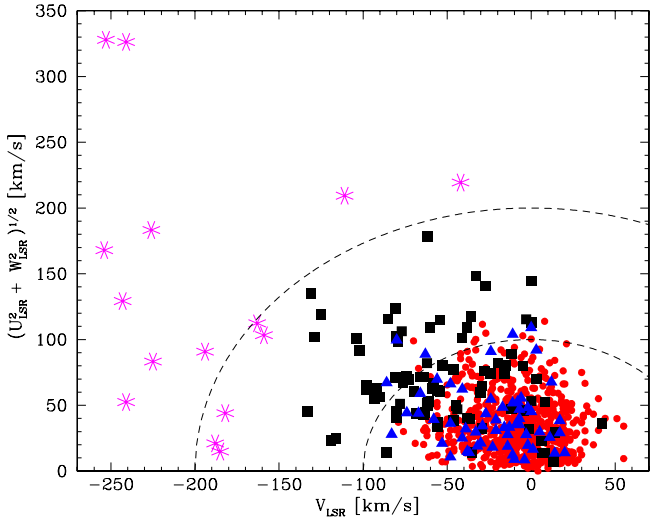

Fig. 3. The Toomre diagram for the entire sample. The symbols are the same as in Fig. 1.

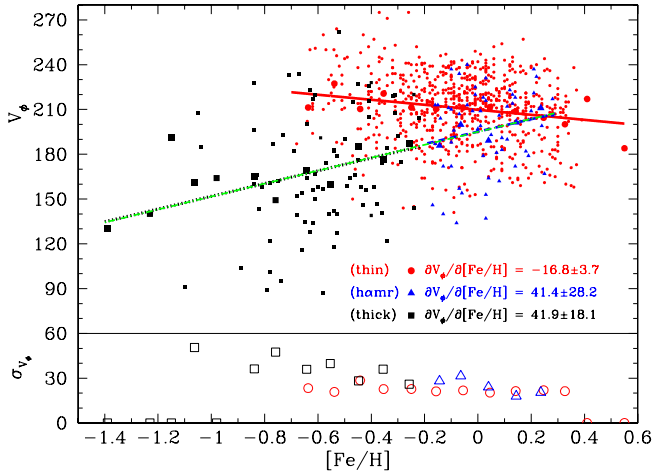

Fig. 4. Galactic rotational velocity gradients (filled symbols) and velocity dispersion gradients (open symbols) with metallicity for stars assigned to different stellar populations. The symbols are the same as in previous plots. The smaller symbols correspond to the real stars and the larger symbols represent the V_ϕ and σ_V values for metallicity bins. Note that the slopes are obtained for the full unbinned data.

little positive or no correlation between V_ϕ and [Fe/H] for stars with high-[α/Fe] i.e., thick disk, old stars (Loebman et al. 2011). Most of the recent observational studies using low-resolution spectra of large samples of thin disk stars outside the solar neighbourhood (mainly farther than 0.5 kpc from the Galactic disk) show a negative gradient of V_ϕ with [Fe/H], which ranges from about –20 to –40 km s^{-1} dex^{-1} (e.g., Lee et al. 2011; Liu & van de Ven 2012; Kordopatis et al. 2011). The magnitude of the gradient also depends on the distance from the Galactic plane (e.g., Lee et al. 2011). Interestingly, a recent study by Navarro et al. (2011) found little or no correlation between V_ϕ and metallicity for their thin disk stars in the solar neighborhood based on a heterogeneous compilation of data from many different sources; their sample also included kinematically selected stars.

To study the degree of radial mixing by exploring the V_ϕ-[Fe/H] correlation, it is important to use a narrow range of galactocentric radii. Otherwise this correlation will appear naturally because of the V_ϕ and metallicity gradients in the Galaxy. Our sample includes stars very close to the Sun (on average ≈45 pc) and is ideal for this search. The top panel of Fig. 4 shows the gradient of mean rotation velocity[5] with metallicity for different groups of stars. The magnitudes of the gradients (the slopes) and the correlation coefficients are presented in Table 2.

The velocity gradient with metallicity obtained for the thin disk stars (–17 km s^{-1} dex^{-1}) is not far from the results (–22 km s^{-1} dex^{-1}) obtained by Lee et al. (2011) for their thin disk stars in the range $0.1 < |Z| < 0.5$ kpc. We note that this steep gradient is in disagreement with the result obtained by Navarro et al. (2011) for solar neighborhood thin disk stars.

Recent studies obtained contradictory results analyzing the V_ϕ gradient with [Fe/H] for the thick disk stars. A steep +40 to +50 km s^{-1} dex^{-1} gradient obtained by Spagna et al. (2010) and Lee et al. (2011) using the SDSS data was confirmed by Kordopatis et al. (2011), who used independent VLT/FLAMES observations of 700 thick disk stars. Other studies (e.g., Ivezić et al. 2008; Bond et al. 2010; Loebman et al. 2011) did not reveal significant correlation probably because of larger errors in the photometric chemical abundances (Lee et al. 2011). We note that all the mentioned studies are based on the samples of stars located far from the Galactic plane (usually $|Z| > 0.5$ kpc).

Figure 4 and Table 2 indicate steep and very similar gradients for the thick disk and for the hαmr stars (about +42 km s^{-1} dex^{-1}). These values agree well with those obtained in Spagna et al. (2010); Lee et al. (2011); and Kordopatis et al. (2011) and, as mentioned before, disagree with the theoretical predictions with radial migration by Schönrich & Binney (2009a) and Loebman et al. (2011). Interestingly, a recent model of chemical enrichment in the Galaxy by Curir et al. (2012) assuming an inverse gradient at high redshifts (z > 3–4) explains the positive rotation-metallicity correlation of the old thick disk population. They showed that by using the inside-out formation and chemical evolution model of the Galactic disk suggested by Matteucci & Francois (1989) and Chiappini et al. (2001), this correlation can be established as a result of radial migration and heating processes of stars from the inner region of the disk.

[5] We adopt 8 kpc for the Sun's distance to the Galactic center and 220 km s^{-1} for the circular velocity of the LSR.

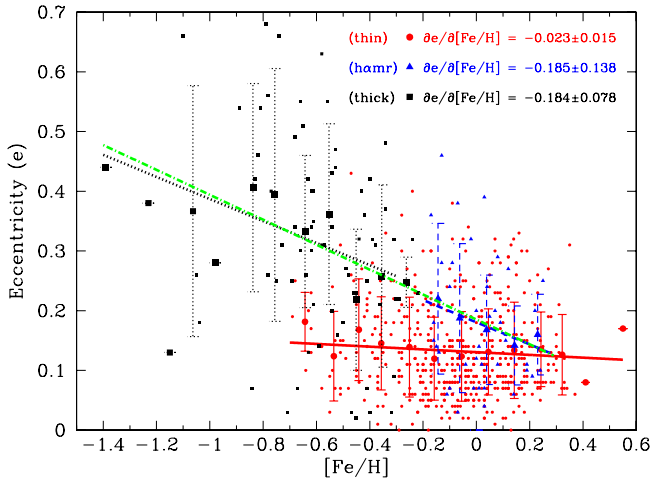

Fig. 5. Trends of eccentricities as a function of metallicity for stars assigned to different stellar populations. The symbols are the same as in previous plots. The smaller symbols correspond to the real stars and the larger symbols present the eccentricities and standard deviations for each metallicity bin. The slopes are again obtained for the unbinned data.

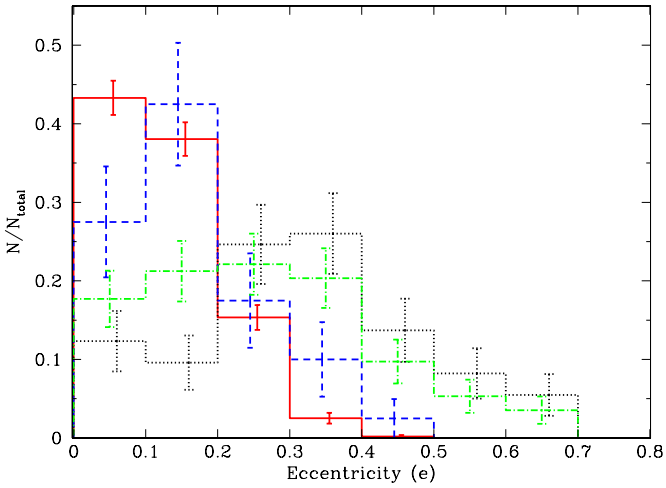

Fig. 6. Normalized distributions of eccentricities for different stellar populations. Designation of the lines kept the same as in the previous plots.

3.2. Stellar orbital eccentricities

The shape of eccentricity (e) distribution of thick disk stars can be used to constrain the main physical mechanism responsible for their formation (Sales et al. 2009). Recent studies (e.g., Dierickx et al. 2010; Wilson et al. 2011; Lee et al. 2011; Kordopatis et al. 2011), which used the Sales et al. (2009) eccentricity test, reached a general conclusion that the eccentricity distribution is inconsistent with the accretion scenario, but could not distinguish between other published models, i.e., heating, migration or merger scenarios.

To discuss the distribution of the stellar orbital eccentricities we cross-matched our sample with the Geneva-Copenhagen Survey sample (Casagrande et al. 2011), which provides the orbital parameters of about 650 stars.

Figure 5 shows trends of e with [Fe/H] for different stellar families and Table 2 presents the observed gradients quantitatively. From Fig. 5 and corresponding table it is obvious that the thick disk and hαmr stars show very similar trends with the same slopes. On the other hand, the trend of the eccentricities for the thin disk stars is practically independent off metallicity. Our results quantitatively agree well with those obtained for the G-type dwarfs from the SDSS/SEGUE survey (Lee et al. 2011).

Figure 6 displays the normalized distributions of eccentricities for the different subsamples. The e distributions of the thin disk stars peak at the first bin (the bin size is 0.1) and has an average value of 0.13. The distribution is also very concentrated around small eccentricities, with only 22 stars (4%) having $e > 0.3$. In contrast, the eccentricity distribution of the thick disk stars has a wider width and peaks at $0.3 < e < 0.4$ bin, with an average value of $e = 0.31$. The eccentricities of the hαmr stars have intermediate values between those of the thin and thick disk stars, with an average value a bit closer to that of the thin disk ($e = 0.17$). In case of hαmr stars again very few stars (5 out of 40) have $e > 0.3$ and only one with $e > 0.4$. Joining the hαmr and thick disk subsamples we obtain an e distribution with a peak at $0.2 < e < 0.3$ and average value of 0.26.

A comparison with the model predictions in Sales et al. (2009) can only rule out the pure accretion scenario (Abadi et al. 2003), while it does not strongly favor or discard any of the other three scenarios. In particular, the shape of the e distribution of the thick disk stars does not differ much from the disk heating model of Di Matteo et al. (2011).

Although the hαmr stars have smaller e compared to the chemically defined thick disk stars, from Fig. 6 it is difficult to conclude that they have different origin or evolution. If the hαmr stars just represent the metal-rich tail of the thick disk, then their smaller eccentricities are a natural consequence of the negative gradient of e with [Fe/H] observed for the thick disk stars (see Fig. 5).

3.3. Significance of the observed trends

To evaluate the statistical significance of the inferred correlations between V_ϕ vs. [Fe/H] and e vs. [Fe/H] we used a bootstrap procedure. First, we obtained the zero-centered distribution of the correlation coefficient by randomly bootstrapping (building random samples by shuffling the parameters among the observed set of parameters) the observed data pairs 10^4 times (see Figueira et al. 2013 for more details). We calculated the correlation coefficient for each of these uncorrelated data sets and then the average and standard deviation of these values. By assuming a Gaussian distribution for $r_{\partial V_\phi/\partial[\mathrm{Fe/H}]}$ ($r_{\partial e/\partial[\mathrm{Fe/H}]}$), we can calculate the probability that the $r_{\partial V_\phi/\partial[\mathrm{Fe/H}]}$ ($r_{\partial e/\partial[\mathrm{Fe/H}]}$) of the original dataset was obtained by pure chance, but we merely present the offset in sigma ($n\sigma(V_\phi)$ and $n\sigma(e)$) in Table 2.

From the table, one can note that the correlations between V_ϕ and [Fe/H] for hαmr and thick disk stars separately are not very significant (1.43σ and 2.24σ), even if the slopes are very steep. Interestingly, the significance of the correlation increases a lot when we consider the thick disk+hαmr sample (5.19σ). To check if this non-significance in both hαmr and thick disk separate samples is due to small sizes of the samples or to small metallicity ranges, we merged the samples in the following way. Since the correlation coefficient (and its significance) does not change if one adds or subtracts a constant to the parameters (in this case to V_ϕ and [Fe/H]), we shifted the thick disk sample (i.e., shifted every point of it) to the *locus* of hαmr stars subtracting the difference between average values of [Fe/H] and V_ϕ of the

thick disk and hαmr stars[6]. This procedure centers both data sets around the same point. Then we calculated the coefficient and significance of the correlation using the same bootstrapping approach. For the merged sample we obtained practically the same slope (41.8 ± 14.6) as for the individual samples and correlation coefficient about 0.234. We found that this correlation is significant at a level of about 2.82σ. If we compare the later value with that obtained for the thick disk subsample we note that by increasing the number of objects in the sample by about 70% we did not increase the significance of the correlation to a great degree. This suggests that the main reason of the obtained low significance is probably the small range of [Fe/H] for independent thick disk and especially for the hαmr subsamples.

We used the same center-shifting approach as we used for the V_ϕ-[Fe/H] data pairs to analyze the significance of the correlation as a function of the size of the thick disk and hαmr subsamples. We found that increasing the size of the subsamples (by about 55% for the thick disk stars) does not greatly increase the significance of the correlations (from 2.24σ to 2.71σ for the thick disk subsample). This is probably, once again, because of the small range of metallicities of the samples.

In our sample we have few thick disk stars with metallicities from –1.4 to –0.9 dex, and these stars are widely spread in this metallicity range. These rather extreme-value stars can influence the fitted slope significantly. From Figs. 4 and 5 one can note that at the lowest metallicities the stars (seven stars with [Fe/H] < -0.9 dex) mostly lie above the V_ϕ-[Fe/H] correlation line and mostly below the e-[Fe/H] correlation line. Interestingly, the much larger data in Lee et al. (2011) suggest similar behavior for their most metal-poor thick disk stars (see Figs. 7 and 9 of Lee et al. 2011). Nevertheless, to check how these data could alter the slopes we established a cut-off in metallicity at [Fe/H] $= -1.1$, -1, and 0.9 dex. We found that the V_ϕ-[Fe/H] slope changes from 48.7 ± 21.9 to 61.5 ± 25.8 km s^{-1} dex^{-1} and the slope of e-[Fe/H] varies from -0.26 ± 0.09 to -0.35 ± 0.11 dex^{-1}. This suggests that when the lower metallicity limit for the thick disk decreases, the slopes become steeper, but stay within the one-sigma errors.

From our tests we can conclude that the observed trends are real, but the exact values of the slopes (for the thick disk) should be considered with caution.

3.4. High-α metal-rich stars

In this section we discuss some properties of the hαmr stellar family that are shared with the thin and thick disk populations.

From Fig. 4 it is interesting to see that although the hαmr and the thin disk stars at [Fe/H] > 0 dex have similar rotation velocities, their trends with metallicity are completely different. The hαmr stars behave like extensions of the thick disk stars on the V_ϕ-[Fe/H] plane, which might mean a similar origin and/or evolution. This similar behavior to the thick disk stars can also be seen in Fig. 5. Although the hαmr stars have orbits with eccentricities that are, on average, more similar to those of the thin disk stars (see Fig. 6), the e vs. [Fe/H] trend of these stars is the same as for the thick disk stars.

Despite the mentioned similarities to the thick disk, the hαmr stars also share some properties of the thin disk. From Table 1 one can see that the dispersion of all the velocity components of hαmr stars is very similar to those of the thin disk sample. In particular the low dispersion of the vertical velocities suggests a short scale-height, very similar to that of the thin disk. Adibekyan et al. (2011) already showed that the average maximum vertical distance (Z_{max}) the stars can reach above the Galactic plane is about 0.3 kpc for the hαmr. For comparison, the average values of Z_{max} are about 0.25 and 1 kpc for the thin disk and thick disk, respectively. Adibekyan et al. (2011) also showed that the hαmr and thick disk family stars have almost the same age, being on average older than thin disk stars by about 3 Gyr. Adibekyan et al. (2012) analyzed the [X/Fe] trends with metallicity of hαmr stars for different elements and showed that for some elements the trends are different than those of the thick disk stars.

At the same time, hαmr stars are more metal-rich than the thick disk stars (if they do not just represent the metal-rich tail of the thick disk) and they are as metal-rich as the bulge stars and have similar enhanced α-element abundances compared to Galactic disk stars as recently found for the bulge stars (e.g., Fulbright et al. 2007; Bensby et al. 2013; Ness et al. 2013)[7].

The mentioned results hint that hαmr stars might have an origin in the inner Galaxy (bulge) and have migrated to the solar annulus (see also Adibekyan et al. 2011; Gazzano et al. 2013). Very recently, in their simulation Roškar et al. (2012) identified a sub-population with high-[Fe/H] and low-[O/Fe]. Although their simulations did not reproduce our data, i.e. separation between low- and high-α stars at super-solar metallicities, at first glance the higher-[O/Fe] part of that family shares many properties of the hαmr stars. From Fig. 7 of Roškar et al. (2012) and Fig. 14 of Loebman et al. (2011)[8] we can see that our hαmr stars match well with the intermediate/old age population of stars with short scale-length and scale-height, migrated from the central part of the Galaxy (<2 kpc).

4. Summary and conclusions

We selected a sample of about 850 solar neighborhood FGK dwarf stars with precise stellar velocity components and chemical abundances derived from the high-resolution HARPS spectra. The stars have $\log g \geq 4$ dex, $5000 \leq T_{\rm eff} \leq 6500$ K, and $-1.4 <$ [Fe/H] ≤ 0.55 dex.

Applying purely chemical approach based on the [α/Fe] vs. [Fe/H] plot, we separate Galactic stellar populations into the thin disk, thick disk, and hαmr. The last two families are separated based on the observed gaps in both [Fe/H] and [α/Fe] distributions. Performing a bootstrapped Monte Carlo test gives a probability higher than 99.99% that the observed gap is statistically significant and is not due to a small-number statistics.

We characterize the stellar subsamples in terms of their kinematics and metallicity and found in general good agreement with earlier determinations of these parameters, although the local normalization for the thin disk is about 82%, which is lower than the usually adopted value (but see also Soubiran et al. 2003; Mishenina et al. 2004; Kordopatis et al. 2011).

Our analysis shows that the rotational velocity of the thin disk stars decreases with increasing [Fe/H] (–17 km s^{-1} dex^{-1}), while this trend shows an increase with [Fe/H] for both thick disk and hαmr, both with the same magnitude of about +42 km s^{-1} dex^{-1}, although the magnitude of the slope for the thick disk stars depends on the cutoff established in [Fe/H].

[6] We note that the slopes of the correlation for the two samples are very similar.

[7] We note that the conclusion that bulge stars are more enhanced in α-elements is also based on Fig. 27 of Bensby et al. (2013), but these authors did not conclude that in their paper.

[8] We note that in both papers they used the same N-body/SPH simulation.

These results, obtained for solar neighborhood stars (on average ≈45 pc), are an independent confirmation of those found for the SDSS sample of stars located far from the Galactic plane (e.g., Lee et al. 2011). The negative gradient of V_ϕ with [Fe/H] for the thin disk agrees well qualitatively with the expectations from the radial migration model, and the steep positive gradients observed for the thick disk and hαmr stars can be explained by the recent simulation by Curir et al. (2012) assuming an inverse chemical gradient in the inner early Galaxy.

For the thin disk stars we observed no correlation between orbital eccentricities and metallicity, but observed a steep negative gradient for the thick disk and hαmr stars with practically the same magnitude of –0.185 dex^{-1}. Again the magnitude of the slope for the thick disk stars depends on the cutoff established in [Fe/H]. These results agree well quantitatively with Lee et al. (2011). The eccentricity distribution of the thin disk subsample suggests that the radial migration played a dominant role in their formation and evolution. From the e distribution of the thick disk stars it is difficult to conclude which mechanism (heating, migration, or merger scenario) played the dominant role, but the peak of the distribution observed at rather lower values than $e \sim 0.5$ and the absence of the secondary peak at higher $e \sim 0.8$ exclude the accretion origin. A combination of two (or more) processes, such as a heating and migration, may describe better the observed distribution, just as it explains the positive rotational velocity gradient with metallicity (Curir et al. 2012).

As previously reported by Adibekyan et al. (2011), there is a family of stars with high [α/Fe] values at solar and super-solar metallicities (see also Gazzano et al. 2013). Although the hαmr stars have intermediate values (even closer to the thin disk) of the orbital parameters and space velocities between thin and thick disks, they show the same behavior as the thick disk stars on the V_ϕ – [Fe/H] and e – [Fe/H] planes. These stars share properties of both the thin and thick disk populations. The properties of the hαmr stars compares well with the metal-rich higher-[O/H] stars in the simulation by Loebman et al. (2011) and Roškar et al. (2012), which have intermediate/old age and are extreme-migrators (probably <1–2 kpc). Based on the mentioned results we are inclined to think that the hαmr stellar family may have originated from the inner Galactic disk/bulge and migrated up to the solar neighborhood, although further investigations are needed to clarify their exact nature.

Acknowledgements. This work was supported by the European Research Council/European Community under the FP7 through Starting Grant agreement number 239953. V.Zh.A., S.G.S., and E.D.M are supported by grants SFRH/BPD/70574/2010, SFRH/BPD/47611/2008, and SFRH/BPD/76606/2011 from the FCT (Portugal), respectively. G.P. is supported by grant SFRH/BPD/39254/2007 and by the project PTDC/CTE-AST/098528/2008, funded by FCT, Portugal. G.I. and J.I.G.H. acknowledge financial support from the Spanish Ministry project MINECO AYA2011-29060, and J.I.G.H. also received support from the Spanish Ministry of Economy and Competitiveness (MINECO) under the 2011 Severo Ochoa Program MINECO SEV-2011-0187. We gratefully acknowledge the anonymous referee for the constructive comments and suggestions. We also thank Helenka Kinnan for the help concerning English.

References

Abadi, M. G., Navarro, J. F., Steinmetz, M., & Eke, V. R. 2003, ApJ, 597, 21
Adibekyan, V. Z., Santos, N. C., Sousa, S. G., & Israelian, G. 2011, A&A, 535, L11
Adibekyan, V. Z., Sousa, S. G., Santos, N. C., et al. 2012, A&A, 545, A32
Anders, E., & Grevesse, N. 1989, Geochim. Cosmochim. Acta, 53, 197
Bensby, T., Feltzing, S., & Lundström, I. 2003, A&A, 410, 527
Bensby, T., Feltzing, S., Lundström, I., & Ilyin, I. 2005, A&A, 433, 185
Bensby, T., Zenn, A. R., Oey, M. S., & Feltzing, S. 2007, ApJ, 663, L13
Bensby, T., Yee, J. C., Feltzing, S., et al. 2013, A&A, 549, A147
Bond, N. A., Ivezić, Ž., Sesar, B., et al. 2010, ApJ, 716, 1
Bovy, J., Rix, H.-W., & Hogg, D. W. 2012a, ApJ, 751, 131
Bovy, J., Rix, H.-W., Liu, C., et al. 2012b, ApJ, 753, 148
Brook, C. B., Gibson, B. K., Martel, H., & Kawata, D. 2005, ApJ, 630, 298
Buser, R., Rong, J., & Karaali, S. 1999, A&A, 348, 98
Casagrande, L. 2012, in Galactic Archaeology: Near-Field Cosmology and the Formation of the Milky Way, eds. W. Aoki, M. Ishigaki, T. Suda, T. Tsujimoto, & N. Arimoto, ASP Conf. Ser., 458, 121
Casagrande, L., Schönrich, R., Asplund, M., et al. 2011, A&A, 530, A138
Chiappini, C., Matteucci, F., & Romano, D. 2001, ApJ, 554, 1044
Curir, A., Lattanzi, M. G., Spagna, A., et al. 2012, A&A, 545, A133
Di Matteo, P., Lehnert, M. D., Qu, Y., & van Driel, W. 2011, A&A, 525, L3
Dierickx, M., Klement, R., Rix, H.-W., & Liu, C. 2010, ApJ, 725, L186
Feltzing, S., & Bensby, T. 2008, Physica Scripta, 133, 4031
Feltzing, S., Bensby, T., & Lundström, I. 2003, A&A, 397, L1
Figueira, P., Santos, N. C., Pepe, F., Lovis, C., & Nardetto, N. 2013, A&A, submitted
Fuhrmann, K. 1998, A&A, 338, 161
Fuhrmann, K. 2008, MNRAS, 384, 173
Fulbright, J. P., McWilliam, A., & Rich, R. M. 2007, ApJ, 661, 1152
Gazzano, J.-C., Kordopatis, G., Deleuil, M., et al. 2013, A&A, 550, A125
Gilmore, G., & Reid, N. 1983, MNRAS, 202, 1025
Haywood, M. 2008, MNRAS, 388, 1175
Ivezić, Ž., Sesar, B., Jurić, M., et al. 2008, ApJ, 684, 287
Ivezić, Ž., Beers, T. C., & Jurić, M. 2012, ARA&A, 50, 251
Jurić, M., Ivezić, Ž., Brooks, A., et al. 2008, ApJ, 673, 864
Kordopatis, G., Recio-Blanco, A., de Laverny, P., et al. 2011, A&A, 535, A107
Kurucz, R. 1993, ATLAS9 Stellar Atmosphere Programs and 2 km s^{-1} grid, Kurucz CD-ROM No. 13, Cambridge, Mass.: Smithsonian Astrophysical Observatory, 13
Lee, Y. S., Beers, T. C., An, D., et al. 2011, ApJ, 738, 187
Liu, C., & van de Ven, G. 2012, MNRAS, 425, 2144
Lo Curto, G., Mayor, M., Benz, W., et al. 2010, A&A, 512, A48
Loebman, S. R., Roškar, R., Debattista, V. P., et al. 2011, ApJ, 737, 8
Matteucci, F., & Francois, P. 1989, MNRAS, 239, 885
Mayor, M., Pepe, F., Queloz, D., et al. 2003, The Messenger, 114, 20
Minchev, I., & Famaey, B. 2010, ApJ, 722, 112
Mishenina, T. V., Soubiran, C., Kovtyukh, V. V., & Korotin, S. A. 2004, A&A, 418, 551
Navarro, J. F., Abadi, M. G., Venn, K. A., Freeman, K. C., & Anguiano, B. 2011, MNRAS, 412, 1203
Ness, M., Freeman, K., Athanassoula, E., et al. 2013, MNRAS, 430, 836
Neves, V., Santos, N. C., Sousa, S. G., Correia, A. C. M., & Israelian, G. 2009, A&A, 497, 563
Nissen, P. E., & Schuster, W. J. 2010, A&A, 511, L10
Nordström, B., Mayor, M., Andersen, J., et al. 2004, A&A, 418, 989
Prochaska, J. X., Naumov, S. O., Carney, B. W., McWilliam, A., & Wolfe, A. M. 2000, AJ, 120, 2513
Quinn, P. J., Hernquist, L., & Fullagar, D. P. 1993, ApJ, 403, 74
Reddy, B. E., Lambert, D. L., & Allende Prieto, C. 2006, MNRAS, 367, 1329
Rix, H.-W., & Bovy, J. 2013 [arXiv:1301.3168]
Robin, A. C., Haywood, M., Crézé, M., Ojha, D. K., & Bienaymé, O. 1996, A&A, 305, 125
Robin, A. C., Reylé, C., Derrière, S., & Picaud, S. 2003, A&A, 409, 523
Roškar, R., Debattista, V. P., Stinson, G. S., et al. 2008, ApJ, 675, L65
Roškar, R., Debattista, V. P., & Loebman, S. R. 2012, MNRAS, submitted [arXiv:1211.1982]
Sales, L. V., Helmi, A., Abadi, M. G., et al. 2009, MNRAS, 400, L61
Santos, N. C., Mayor, M., Bonfils, X., et al. 2011, A&A, 526, A112
Schönrich, R., & Binney, J. 2009a, MNRAS, 396, 203
Schönrich, R., & Binney, J. 2009b, MNRAS, 399, 1145
Sellwood, J. A., & Binney, J. J. 2002, MNRAS, 336, 785
Sneden, C. A. 1973, Ph.D. Thesis, The university of Texas at Austin
Soubiran, C., Bienaymé, O., & Siebert, A. 2003, A&A, 398, 141
Sousa, S. G., Santos, N. C., Israelian, G., Mayor, M., & Monteiro, M. J. P. F. G. 2007, A&A, 469, 783
Sousa, S. G., Santos, N. C., Mayor, M., et al. 2008, A&A, 487, 373
Sousa, S. G., Santos, N. C., Israelian, G., et al. 2011a, A&A, 526, A99
Sousa, S. G., Santos, N. C., Israelian, G., Mayor, M., & Udry, S. 2011b, A&A, 533, A141
Spagna, A., Lattanzi, M. G., Re Fiorentin, P., & Smart, R. L. 2010, A&A, 510, L4
Tsantaki, M., Sousa, S. G., Adibekyan, V. Z., et al. 2013, A&A, in press DOI: 10.1051/0004-6361/201321103
Udry, S., Mayor, M., Naef, D., et al. 2000, A&A, 356, 590
Villalobos, Á., & Helmi, A. 2008, MNRAS, 391, 1806
Wilson, M. L., Helmi, A., Morrison, H. L., et al. 2011, MNRAS, 413, 2235